Archaeol Anthropol Sci (2017) 9:197–208
DOI 10.1007/s12520-015-0270-3

ORIGINAL PAPER

FTIR imaging and HPLC reveal ancient painting and dyeing techniques of molluskan purple

Zoi Eirini Papliaka[1] · Alexandros Konstanta[2] · Ioannis Karapanagiotis[2] · Recep Karadag[3,4] · Ali Akin Akyol[5] · Dimitrios Mantzouris[6] · Panagiotis Tsiamyrtzis[7]

Received: 11 June 2015 / Accepted: 15 July 2015 / Published online: 26 July 2015

Abstract Fourier transform infrared spectroscopy and imaging coupled to optical microscopy, scanning electron microscopy coupled to energy dispersive x-ray spectroscopy and high-performance liquid chromatography (HPLC) coupled to diode-array detection are used to investigate two samples removed from a painted decoration of a burial kline and a textile fragment, both found in Koru tumulus (fifth century BCE) in Daskyleion. Tyrian purple and kaolinite were identified in both samples, thus suggesting that the aluminosilicate compound had an important role in the applied painting and dyeing processes. The textile fragment is composed of undyed cotton and silk yarns dyed with the molluskan dye. The relative compositions of the molluskan materials used in the two archaeological objects are similar and comparable with the corresponding composition measured for a purple sample originated from *Murex trunculus* mollusks according to the HPLC results. This result is supported by principal component analysis (PCA) which, furthermore, takes into account the relative compositions of the extracts of the three Mediterranean mollusks, published in previous reports.

Keywords FTIR · Imaging · HPLC · Tyrian purple · Murex · Kaolinite

✉ Ioannis Karapanagiotis
y.karapanagiotis@aeath.gr

[1] Elettra Sincrotrone Trieste S.C.p.A., AREA Science Park, Basovizza, Trieste, Italy

[2] Department of Management and Conservation of Ecclesiastical Cultural Heritage Objects, University Ecclesiastical Academy of Thessaloniki, Thessaloniki, Greece

[3] Laboratory for Natural Dyes, Marmara University, Istanbul, Turkey

[4] Turkish Cultural Foundation, Cultural Heritage Preservation and Natural Dyes, Istanbul, Turkey

[5] Department of Conservation & Restoration of Cultural Properties, Gazi University-Faculty of Fine Arts, Ankara, Turkey

[6] Ormylia Foundation, Art Diagnosis Center, Ormylia, Greece

[7] Department of Statistics, Athens University of Economics and Business, Athens, Greece

Introduction

The development of multi-analytical strategies, which include the use of complementary techniques, to identify dyes and pigments in archaeological findings is important for two reasons. First, thorough strategies can be implemented to study different types of objects where colourants were applied in different ways, e.g. paints, textiles etc. Second, multi-analytical strategies can provide a better understanding on the identity and moreover the ancient application process of a dye or pigment.

Non-destructive techniques (NDTs) have an inherent advantage which is the preservation of samples removed from an archaeological object. Herein, the term 'non-destructive' means precisely that a sample is not consumed in any way by the analysis performed using a NDT. Complementary NDTs can, in principle, be used to characterise both inorganic and organic colourants and other materials, thus providing a thorough understanding of ancient painting and dyeing recipes. However, if an organic colourant is present in the archaeological sample, then the application of separation, chromatographic methods is usually necessary to achieve a detailed characterisation. Chromatography can easily provide quantitative results for the compounds detected in an archaeological sample. This can be extremely important to identify the exact

biological source of a dye, as it was shown, for instance, for cochineal (Serrano et al. 2011; Wouters and Verhecken 1989), madder (Wouters 2001), dragon's blood (Sousa et al. 2008) and Tyrian purple (Karapanagiotis et al. 2013; Koren 2008) species. Mass spectrometric techniques are also very useful for dye characterisation and can provide important information about the structures of the dye molecules (Mantzouris et al. 2011; Michel et al. 1992a, 1992b).

The study presented herein aims at characterising the materials contained in two samples removed from two objects found within a tomb. The burial monument was excavated in the archaeological area of Daskyleion and more precisely in the Koru tumulus (İren 2012, 2013). Samples were removed from the purple painted surface of a kline (couch) and a purple textile fragment both dated to the fifth century BCE. Fourier transform infrared spectroscopy coupled to optical microscopy (micro-FTIR), scanning electron microscopy (SEM) coupled to energy dispersive x-ray (EDX) spectroscopy and Fourier transform infrared imaging (FTIRI) compose the group of the NDTs which are applied to reveal the use of Tyrian purple and moreover to obtain interesting results related to the painting and dyeing processes applied on the objects. This is the first report where FTIRI is used to study samples containing the royal purple. High-performance liquid chromatography coupled to diode-array detection (HPLC-DAD) is used to characterise in detail the purple pigment and dye used in the kline and textile, respectively. The chromatographic results of the two archaeological samples are compared with HPLC data of the literature (Karapanagiotis et al. 2006, 2013; Koren 1995, 2008; Mantzouris and Karapanagiotis 2014; Nowik et al. 2011; Wouters 1992) which describe the relative compositions of the three Mediterranean molluskan species, that is *Hexaplex trunculus* L. (*Murex trunculus*), *Bolinus brandaris* L. (*Murex brandaris*) and *Stramonita haemastoma* (*Thais haemastoma*). The comparison is carried out using principal component analysis (PCA).

The unequivocal identification of Tyrian purple in archaeological findings using chemical methods is rare. For the period of interest (around fifth century BCE), Tyrian purple was identified in three objects found in the Eastern Mediterranean: in the Persian King Darius I stone jar dated in the fifth century BCE (Koren 2008), in a fabric found within a sarcophagus (fifth century BCE) which was excavated in Athens, Greece (Margariti et al. 2013) and an astragalos (sixth to second century BCE) found in the cave of Koroneia, Greece (Colombini et al. 2004). Mediterranean archaeological findings decorated with molluskan purple and dated to the later Macedonian and Hellenistic periods are also rare (Andreotti et al. 2006; Kakoulli 2002; Karydas 2006; Maravelaki-Kalaitzaki and Kallithrakas-Kontos 2003).

Materials and methods

Samples

The Koru tumulus in Daskyleion (Fig. 1), Turkey, has a long corridor (dromos), an antechamber and a main grave chamber dated to the fifth century BCE according to silver coins and other archaeological objects found within the monument (İren 2012, 2013). Two Lydian-type klinai (couches), found in the main chamber, have purple decoration on their outer surfaces. A sample was removed from this remaining purple surface. Another sample was removed from a purple textile fragment found within the burial monument.

Purple material, used as a reference in comparison to the two archaeological samples, was produced from fresh *Murex trunculus* mollusks which were collected in the Thermaic gulf, along the coastline of Thessaloniki, Greece. This molluskan sample was analysed only by HPLC.

Compounds in pure form used as standards for identification purposes were indigotin (IND) which was purchased from Fluka, indirubin (INR), 6-bromoindigotin (MBI), 6′-bromoindirubin (6′MBIR), 6-bromoindirubin (6MBIR), 6,6′-dibromoindigotin (DBI) and 6,6′-dibromoindirubin (DBIR) which were synthesised in a previous study (Karapanagiotis et al. 2013). The brominated molecules are contained only in Tyrian purple. However, as DBI was the first compound which was identified in Tyrian purple (Friedländer 1909), it is usually taken as the marker compound for identification purposes.

Microscopy and EDX

Samples were studied using a Zeiss Axioskop 40 polarising light microscope equipped with a UV source and scanning electron microscopy (SEM, JEOL, JSM-6510) with energy-dispersive x-ray spectroscopy (EDX; Swift-ED, Oxford). For the SEM and SEM-EDX studies, samples were coated with a thin layer of carbon.

FTIR microspectroscopy and imaging

Sample preparation

Small parts of interest were separated from the archaeological samples, positioned and pressed with a diamond anvil cell device, so as thin sections to be prepared. The diamond anvil cell device (Tucson) is designed to flatten a sub-millimetre-sized sample by compressing it between opposing diamond culets. A thinner section allows maximum transmission of the IR radiation enabling to obtain sharp, well-resolved spectra. After the sample was compressed, the facet containing the flattened sample was placed directly on the motorised stage of the Vis-IR microscope (Derrick et al. 1999).

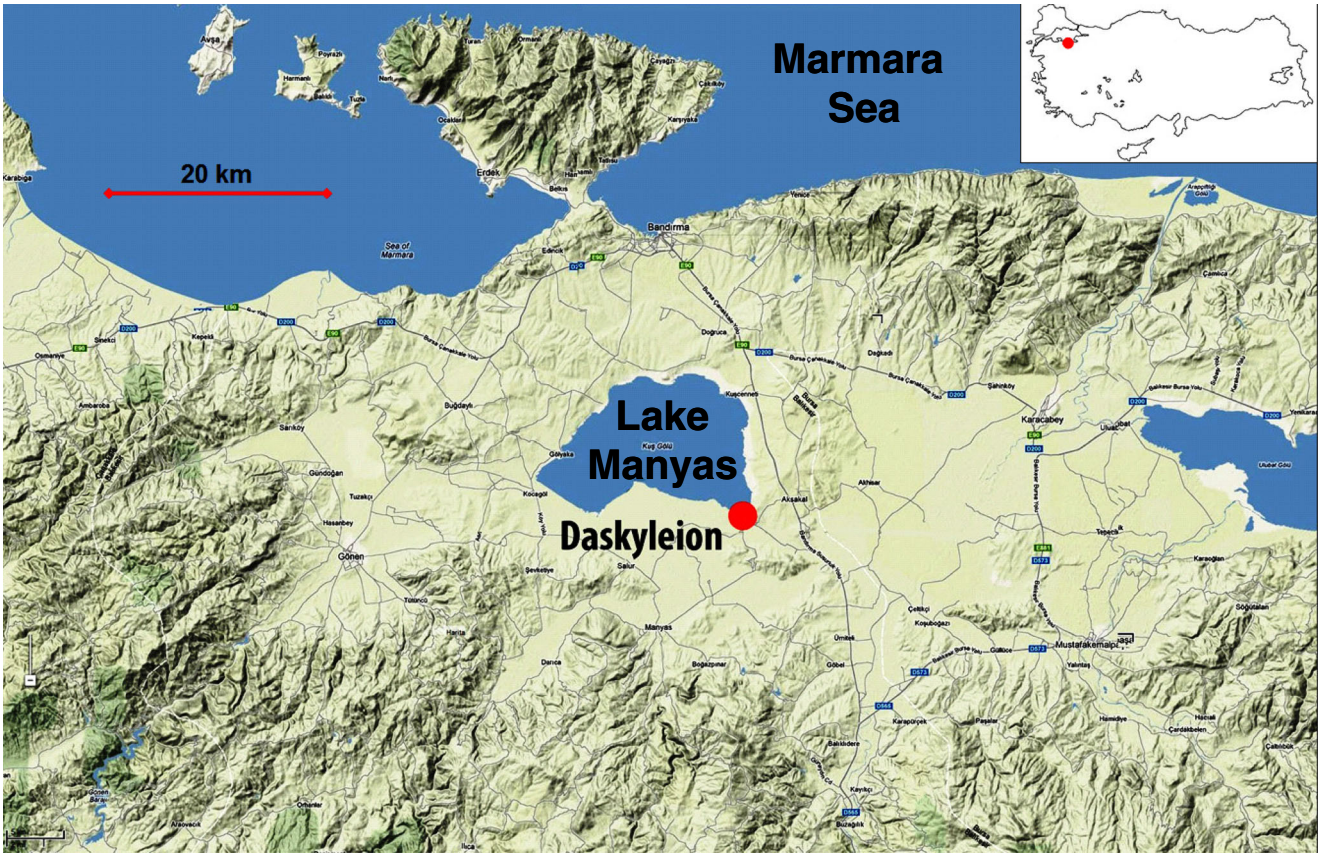

Fig. 1 The location of the archaeological site of Daskyleion

Instrumentation

The samples were studied at SISSI beamline at Elettra—Sincrotrone Trieste, which is equipped with a Bruker VERTEX 70 FTIR spectrometer coupled with the Hyperion 3000 Vis/IR microscope. Analyses were performed using the conventional IR source of the Bruker instrument. Single-point analyses were followed by FTIR chemical images which were collected in selected areas of interest. Infrared spectra (single-point analysis) were recorded using the MCT detector in transmission mode. For each sample, 15–20 spectra were collected in the range of 4000–700 cm^{-1} with a spectral resolution of 4 cm^{-1}, an aperture size of 25×25 μm^2 and averaging 256 scans per spectrum.

To obtain information on the spatial distribution of the chemical compounds (FTIR chemical images), samples were measured in transmittance with a projected pixel size ~2.56 μm, using a Focal Plane Array (FPA) detector (64×64 detector elements) and a 15× condenser/objective (NA=0.4) arrangement. Spectra were collected with 8 cm^{-1} spectral resolution in the range of 4000–900 cm^{-1} and co-adding 256 scans. The size of individual FTIR images is approximately 170×170 μm^2. The magenta and the blue false colours in FTIR images denote high and low absorbance, respectively.

HPLC

Chemicals

HPLC-grade dimethyl sulfoxide (DMSO; Sigma-Aldrich) was used for sample preparation. Chromatography was operated using type I reagent-grade water with resistivity up to 18.3 MΩ/cm and organic content less than 5 ppb, produced by a Barnstead EASYpure water purification system, HPLC-grade acetonitrile (CH_3CN; J. T. Baker) and trifluoroacetic acid (TFA; Riedel-de Haën) of 99 % purity.

Sample preparation

Purple material was produced from fresh *M. trunculus* mollusks as follows. The hypobranchial glands were removed from the shells of the mollusks and exposed to direct sunlight for 3 h. The glands became coloured and were dissolved in DMSO which was heated at 80 °C for 30 min.

Warm DMSO (80 °C) bath was used to treat the paint and textile archaeological samples to extract the contained Tyrian purple. The extraction method is described in detail elsewhere (Karapanagiotis et al. 2013).

The aforementioned DMSO solutions were subjected to centrifugation and the upper clear phases were analysed by HPLC.

Instrumentation

The HPLC-DAD system (Thermoquest) consisted of a 4000 quaternary HPLC pump, a SCM 3000 vacuum degasser, an AS3000 auto sampler with column oven, a Rheodyne 7725i Injector with 20 μL sample loop and a Diode Array Detector UV 6000LP. Analyses were carried out with an Alltima HP C18 5 μm column with dimensions 250×3.0 mm (Alltech) at a stable temperature of 35 °C. The monitoring wavelength was 288 nm. The gradient elution program was consisted of H_2O+ 0.1 % TFA and CH_3CN+0.1 % TFA (Karapanagiotis et al. 2013).

Results and discussion

Microscopic and spectroscopic results for the paint sample

Figure 2a and b shows the main chamber of the Koru tumulus and a detail of the remaining purple decoration on the surface of a kline. A sample (Fig. 2c) was extracted and was first investigated using single-point FTIR analysis. The distinctive spectrum of Tyrian purple (3380, 1634, 1615, 1577, 1445, 1388, 1314, 1281, 1244, 1201, 1158, 1106, 1081, 1048 and 900 cm^{-1}) (Clark and Cooksey 1999) is revealed in Fig. 2d pointing out its dominant presence at the bright purple regions of the sample. Identification is demonstrated by comparing the spectrum collected for the archaeological sample (solid line in Fig. 2d) with the spectrum of reference DBI (dashed line in Fig. 2d). In particular, the spectra of both samples show the

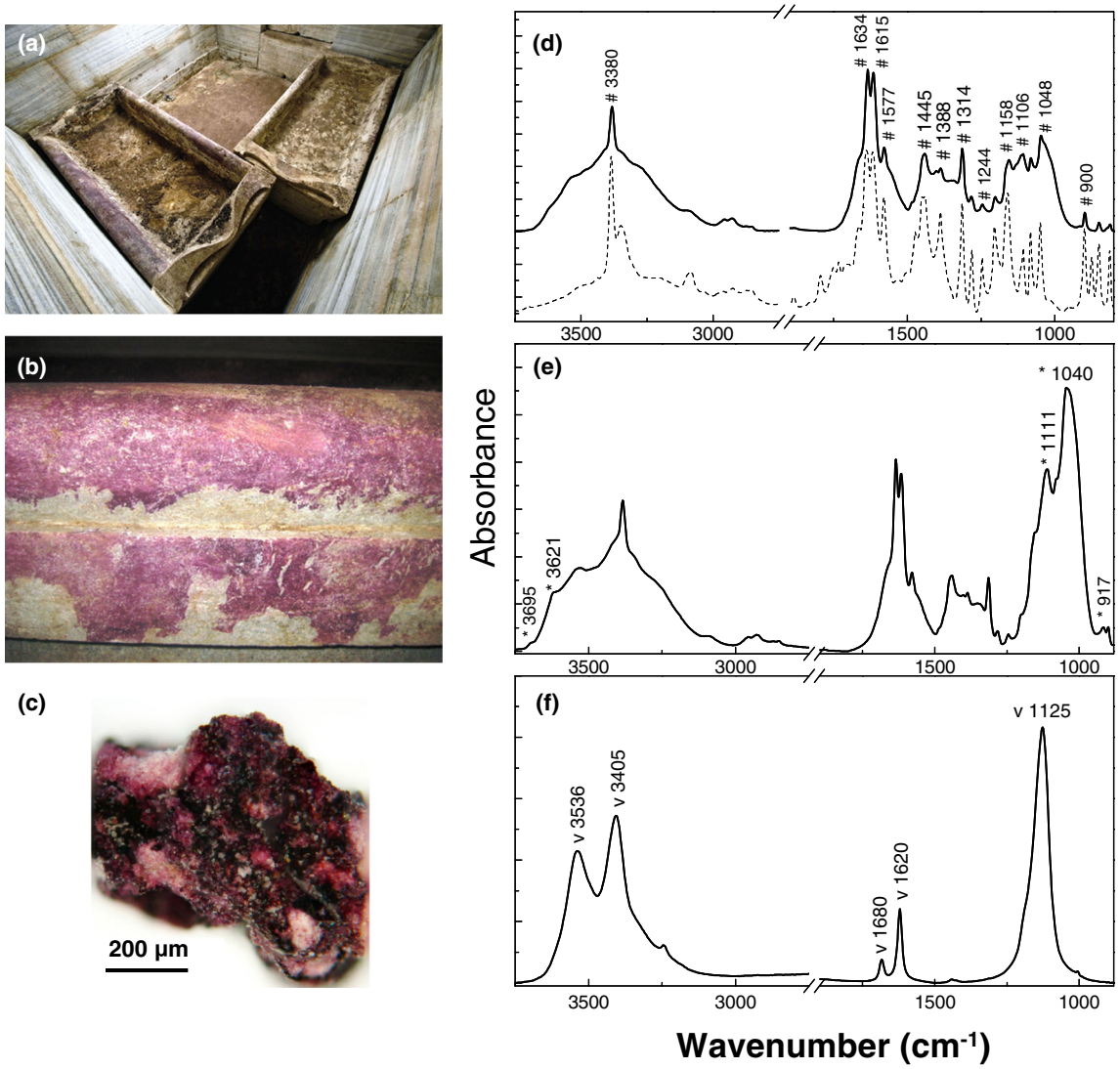

Fig. 2 **a** The main chamber of the Koru tumulus in Daskyleion with the two klinai. **b** Detail of purple decoration. **c** Sample extracted from the painted decoration. FTIR spectra taken from different regions of the purple material revealing the presence of **d** Tyrian purple (#, *solid line*), **e** kaolinite (*asterisks*) and **f** gypsum (*v*). For comparison, the spectrum of reference DBI is provided in (**d**) (*dashed line*)

characteristic peaks at ca. 3380 cm^{-1} (NH stretch), ca. 1634 cm^{-1} (C=O stretch) and ca. 1577 cm^{-1} (C=C stretch) (Clark and Cooksey 1999). Apparently, FTIR analysis reveals the presence of Tyrian purple in the studied archaeological sample, but it cannot distinguish the various components of the purple paint, a task which is achieved by HPLC, as discussed later. Moreover, kaolinite, $Al_2Si_2O_5(OH)_4$ (3695, 3621, 1111, 1040 and 917 cm^{-1}), and gypsum, $CaSO_4 \cdot 2H_2O$ (3536, 3405, 1680, 1620 and 1125 cm^{-1}), were detected in the paint sample, according to results of Fig. 2e and f, respectively (Derrick et al. 1999).

The aforementioned identifications were confirmed by SEM-EDX results presented in Fig. 3. The detection of Br is indicative for the use of true purple in the archaeological sample. Furthermore, the presence of an aluminosilicate compound and gypsum is supported by the results of Fig. 3 as Al, Si, Ca and S are included in the detected elements of the EDX spectrum.

FTIR imaging was carried out throughout a selected region of the purple painted material (Fig. 4a). The chemical image created by integrating the C=C stretching band at 1577 cm^{-1} (Clark and Cooksey 1999) exhibits the distribution of Tyrian purple and is presented in Fig. 4b. This spectral absorption band was selected for plotting the distinctive FTIR image of Tyrian purple as its frequency is the most appropriate to distinguish the purple paint from the other materials contained in the sample. The archaeological sample is rich in kaolinite and gypsum, as it can be appreciated by integrating the Si–O stretching band at 1040 cm^{-1} (Fig. 2e) and the O–H bending band at 1680 cm^{-1} (Fig. 2f) shown in Fig. 4c and d, respectively.

The identification of kaolinite is interesting and could be important for the paint recipe technology applied on the klinai. Past research on the preparation procedure of Tyrian purple, when this was used as a paint, proved the chalk base of Tyrian purple, rich in aragonite, indicating that it was probably obtained by crushed sea shells, as aragonite is typically found in crystals developed in sea environment (Karapanagiotis et al. 2004; Sotiropoulou and Karapanagiotis 2006). Moreover, the presence of chalk in raw form (calcite) was interpreted as ultimately added to the purple dried material and ground together to give body to the pigment and lighten its colour before applying it to the wall (Karapanagiotis et al. 2004; Sotiropoulou and Karapanagiotis 2006). However, aragonite included in the paint technology of Tyrian purple of the Minoan period was not detected herein. Instead of calcium carbonate, kaolinite was detected in Figs. 2, 3 and 4.

Mineralogical analysis of a sample removed from a purple stain at the outer surface of the Darius I stone jar, suggested that kaolinite may have been used on the coloured stain (Westenholz and Stolper 2002) which was painted with Tyrian purple according to a later HPLC investigation (Koren 2008). The unequivocal identification of kaolinite was not reported (Westenholz and Stolper 2002), but its presence was speculated and supported by the mineralogical results which showed that elevated amounts of Al and Si were present at the stained area. Interestingly, the Darius I jar is dated in the fifth century BCE and therefore is contemporary to the Koru tumulus. Consequently, the use of kaolinite in the Tyrian purple paint technology could be indicative for this historical period.

Microscopic and spectroscopic results for the textile sample

Figure 5a and b shows microphotographs under visible and UV light, respectively, of the textile sample. It is seen that the textile fragment is composed of undyed and purple dyed

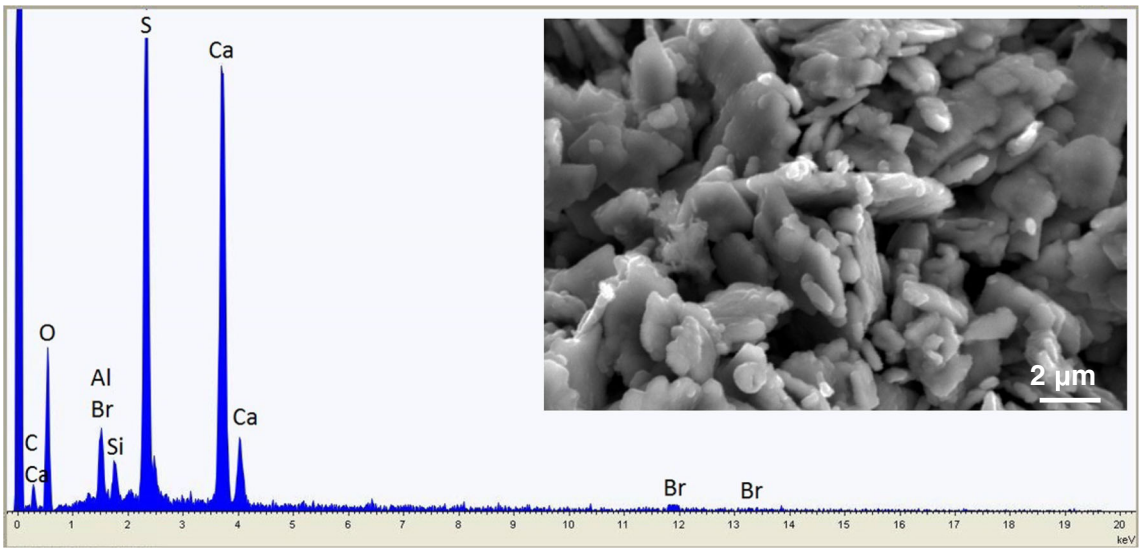

Fig. 3 SEM image of the paint sample and EDX spectrum

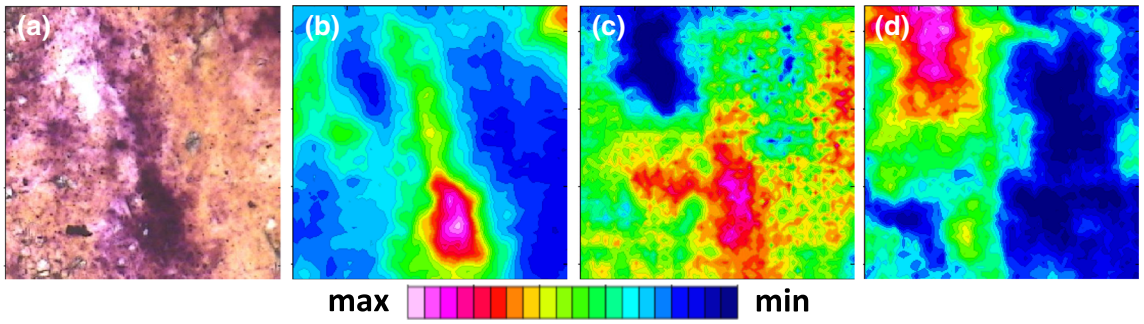

Fig. 4 **a** Visible image in transmission, taken from a region of the paint sample, which was selected for FTIR imaging in transmission mode, after being pressed with the diamond anvil cell device. FTIR images, representing the peak areas at **b** 1577 cm^{-1}, spatial distribution of Tyrian purple; **c** 1040 cm^{-1}, spatial distribution of kaolinite; and **d** 1680 cm^{-1}, spatial distribution of gypsum. The size of the FTIR images is 170×170 μm^2

yarns, probably corresponding to warps and wefts, respectively. Figure 5c shows a SEM image of an undyed yarn. The longitudinal morphology of the fibres, such as the helicoidal twisting and swelling along the fibre axis due to the absence of moisture, is characteristic for the *Gossypium* species (cotton) (Cook 1993; Graves and Saville 1995; Luniak 1953).

The cellulosic nature of the undyed yarns is spectroscopically identified in Fig. 6. Undyed yarns of the textile fragment were pressed with the diamond anvil cell device (Fig. 6b) and subsequently studied with FTIR, performing initially single-point analysis. The IR spectrum shown in Fig. 6a reveals the cellulosic nature of the undyed yarns (broad ~3600–3200, 2900, 1645, 1430, 1372, 1315, 1202, 1160, 1112, 1060, 1036 and 900 cm^{-1}). The bands in the region 1300–1400 cm^{-1} (COH and HCC bending) are typical of crystalline cellulose, whereas the absence of the band at 1335 cm^{-1} in the spectrum is due to biodegradation process (Kavkler et al. 2011). Both bands at 1430 (CH_2 bending) and 1111 cm^{-1} (C–O–C stretching) are characteristic of crystalline cellulose I. On the contrary the band at 900 cm^{-1} is indicative of the amorphous cellulose. In the literature, the band at 1430 cm^{-1} is assigned as 'crystalline' and at 900 cm^{-1} as 'amorphous' (Kavkler et al. 2011). Consequently, by integrating the 'crystalline' band at 1430 cm^{-1} and the 'amorphous' band at 900 cm^{-1}, the crystalline structure of the cellulosic fibre is attested at Fig. 6c and d.

A part of the purple dyed fibrous material was pressed with the diamond anvil cell device and studied with FTIR. The recorded IR spectra taken from different areas of the sample pointed out the presence of proteinaceous fibres (broad ~3500–3200, 3080, 1655, 1540, 1400, 1344, 1235 and 1167 cm^{-1}) (XiaoMei and Paul 2010) which were dyed with Tyrian purple (3380, 1634, 1577, 1440, 1314, 1158, 1106 and 900 cm^{-1}) and were also treated with kaolinite, $Al_2Si_2O_5(OH)_4$ (3695, 3621, 1111, 1040 and 917 cm^{-1}), as shown in Fig. 7a, b and c, respectively. In particular, the bands at 1655 cm^{-1} (amide I) and 1540 cm^{-1} (amide II) shown in Fig. 7a are slightly shifted to higher frequencies, which might witness the presence of sericin gum which cements together the fibroin filaments. The amide I and II peaks of sericin appear at ca. 1650 and ca. 1530 cm^{-1}, respectively, as opposed to ca. 1625 and ca. 1520 cm^{-1} for fibroin (XiaoMei and Paul 2010). Moreover, the peak at 1400 cm^{-1}, present in the spectrum of Fig. 7a, is a further signature peak of sericin, whereas the other characteristic peak of sericin at 1070 cm^{-1} is masked by the broad absorption of kaolinite at the same spectral range. The broad absorbance at ~3350 cm^{-1} is due to associated water and the raised hydroxyl content. Silk is usually degummed, a procedure based on the distinct properties of the two proteins, namely the water soluble nature of sericin, compared to the insolubility of fibroin. However, in the case of the fibrous archaeological material under study, the

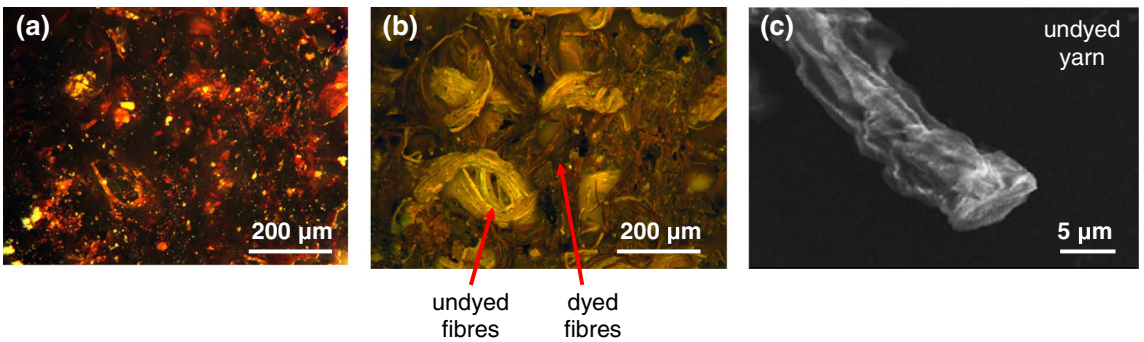

Fig. 5 Area of the textile sample in **a** visible and **b** UV light, revealing the presence of undyed and dyed fibres. **c** SEM image of an undyed yarn

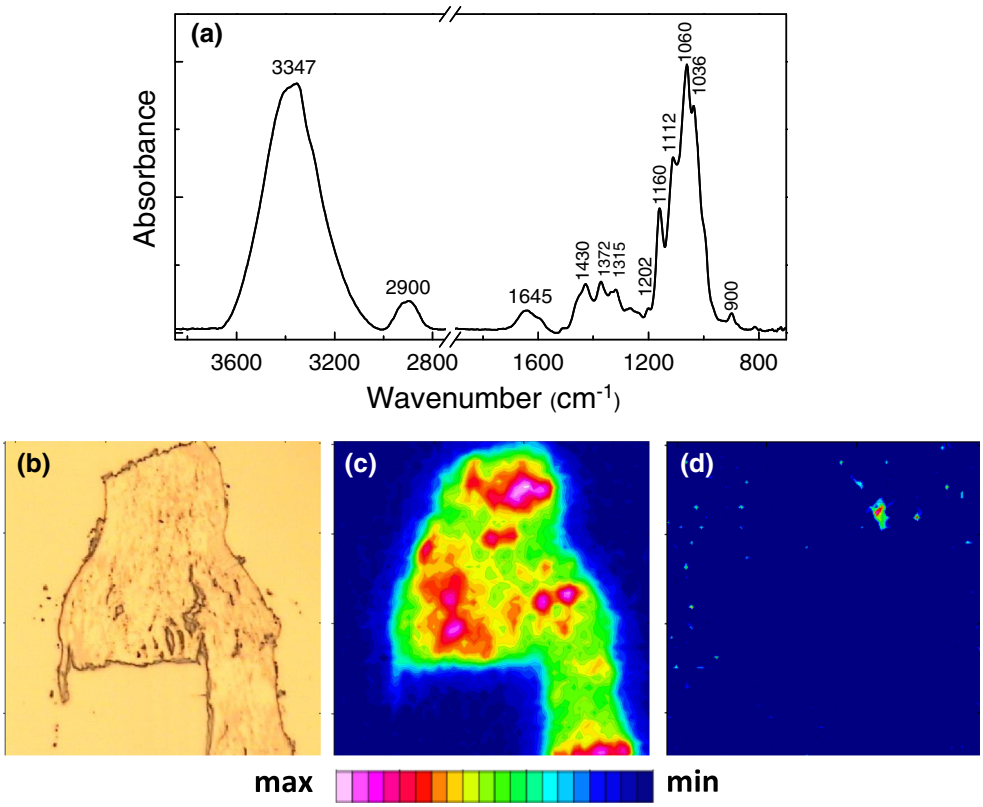

Fig. 6 **a** FTIR spectrum taken from undyed yarns of the textile sample, revealing their cellulosic nature. **b** Visible image in transmission, taken from an undyed region of the textile sample, which was selected for FTIR imaging in transmission mode, after being pressed with the diamond anvil cell device. FTIR images representing the peak areas at **c** 1430 cm^{-1}, characteristic of the crystalline cellulose I form, and **d** 900 cm^{-1}, characteristic of the amorphous cellulose. The size of the FTIR images is 170×170 μm^2

degummed procedure may have not taken place (XiaoMei and Paul 2010).

Elemental analysis carried out by SEM-EDX on the purple dyed yarns offered support to the identification of Tyrian purple and kaolinite, described above. In the EDX spectrum of Fig. 8, Br can be assigned as marker element for the identification of true purple. Al and Si are originated from kaolinite which often contains oxides of Mg (Nour and Awad 2008).

The FTIR image plotted by integrating the amide II (C–N–H) bending band at 1540 cm^{-1} throughout a region of the purple fibrous archaeological material (Fig. 9a) shows the proteinaceous nature of the textile substrate (Fig. 9b) and coincides with the chemical image of sericin, obtained by plotting its characteristic peak at 1400 cm^{-1} (Fig. 9c). The chemical image corresponding to Tyrian purple is shown in Fig. 9d and was obtained by integrating its characteristic band at 1314 cm^{-1}, which can be clearly observed and distinguished from the spectrum of the proteinaceous fibre. The C=C stretching band at 1577 cm^{-1} could not be selected, as previously, for plotting an accurate FTIR image of the Tyrian purple, as it cannot be easily distinguished from the amide II (C–N–H) bending band appearing at the same spectral range. The FTIR image for kaolinite is shown in Fig. 9e and was obtained by integrating the silicate absorption band at 1040 cm^{-1}. To the best of our knowledge, this is the first report that reveals the use of kaolinite in the ancient textile technology of Tyrian purple. As kaolinite was identified also in the paint sample, it can be suggested that the aluminosilicate compounds might have had an important role whenever Tyrian purple was applied on either textiles or stones. The use of kaolinite could aim at providing body to the pigment (case of paint sample) and/or producing a ground layer for the application of the purple colourant (cases of paint and textile samples). This may imply that a different technique than the standard vat dyeing process (Cardon 2007; McGovern and Michel 1990) might have been applied on the textile of the Koru tumulus. Moreover, the images in Fig. 9e and d suggest that kaolinite is distributed throughout the entire fibrous matter and its higher intensity (magenta false coloured) area, namely its higher concentration area, does not concur with the higher intensity area of Tyrian purple. This result offers support to the argument that the treatment of the textile fibres with kaolinite probably constituted a different stage, which might prelude the dyeing process with Tyrian purple.

Chromatographic results

The chromatograms collected for the paint and textile archaeological samples are shown in Fig. 10a and b, respectively. Figure 10c shows the chromatogram collected for the purple material obtained from fresh *M. trunculus* mollusks. The relative (%) HPLC peak areas at 288 nm are summarised in the inset table of the figure.

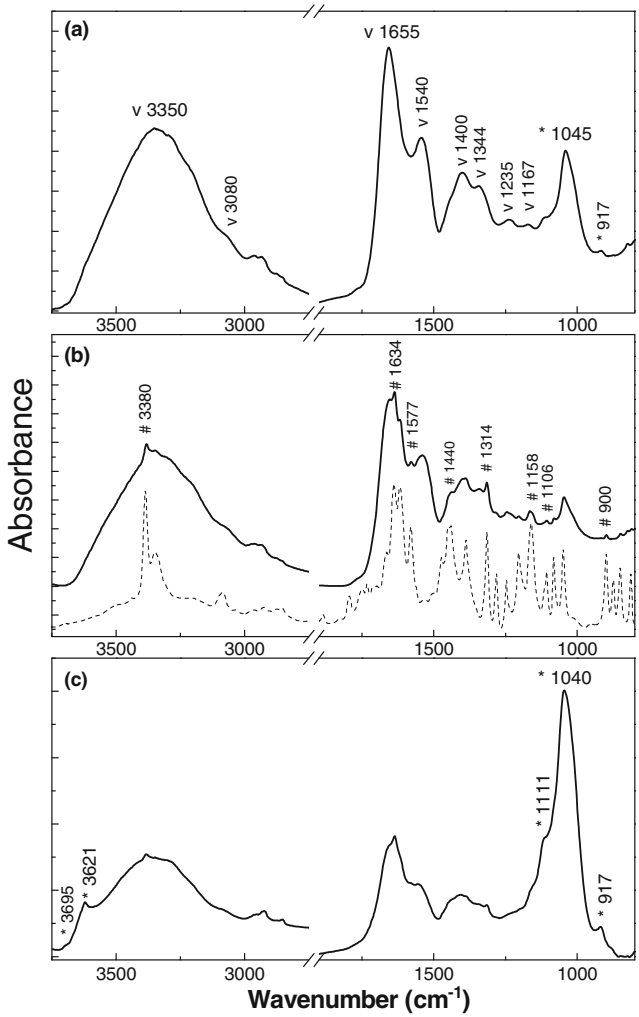

Fig. 7 FTIR spectra taken from different regions of purple yarns of the textile sample revealing **a** their proteinaceous nature (*v*), **b** the presence of Tyrian purple (#, *solid line*) and **c** kaolinite (*asterisks*). For comparison, the spectrum of reference DBI is provided in (**b**) (*dashed line*)

The chromatograms of the two archaeological samples are qualitatively similar. Both samples are rich in MBI and DBIR, and contain considerable amounts of IND and DBI and low amounts of INR and its monobrominated derivatives, 6′MBIR and 6MBIR. Consequently, it can be argued that similar methods and/or molluskan sources may have been applied and used to treat the two samples. The extract of the *M. trunculus* reference sample corresponds to high amounts of MBI and DBIR and elevated amount of DBI, as reported for the two archaeological samples. Interestingly, the reference sample is poor in IND which is not usually the case for extracts of *M. trunculus* mollusks (Karapanagiotis et al. 2006, 2013; Koren 2008; Wouters 1992). *M. trunculus* mollusks poor in IND were rarely reported (Koren 1995, 2008). Overall, the HPLC graph and the relative composition of the *M. trunculus* sample are not that different than the corresponding data reported for the two archaeological samples. To support this observation, a covariance-based PCA analysis was carried out to compare the HPLC peak areas measured for the two archaeological samples with corresponding data reported previously for the three Mediterranean molluskan species, that is *M. trunculus*, *M. brandaris*, and *T. haemastoma*. Previously reported HPLC peak areas measured at 288 nm (Karapanagiotis et al. 2006, 2013; Koren 1995, 2008; Mantzouris and Karapanagiotis 2014; Nowik et al. 2011; Wouters 1992) for purple mollusks are summarised in Table 1 and used to construct the PCA plot. Monobromoindirubins were usually not reported in old investigations and therefore the available compositional data for 6′ MBIR and 6MBIR are extremely rare. Consequently, these two compounds are eliminated from Table 1 and our consideration for the PCA analysis.

In a previous study, it was shown that the PCA plot is effective to separate *M. trunculus* from the other two

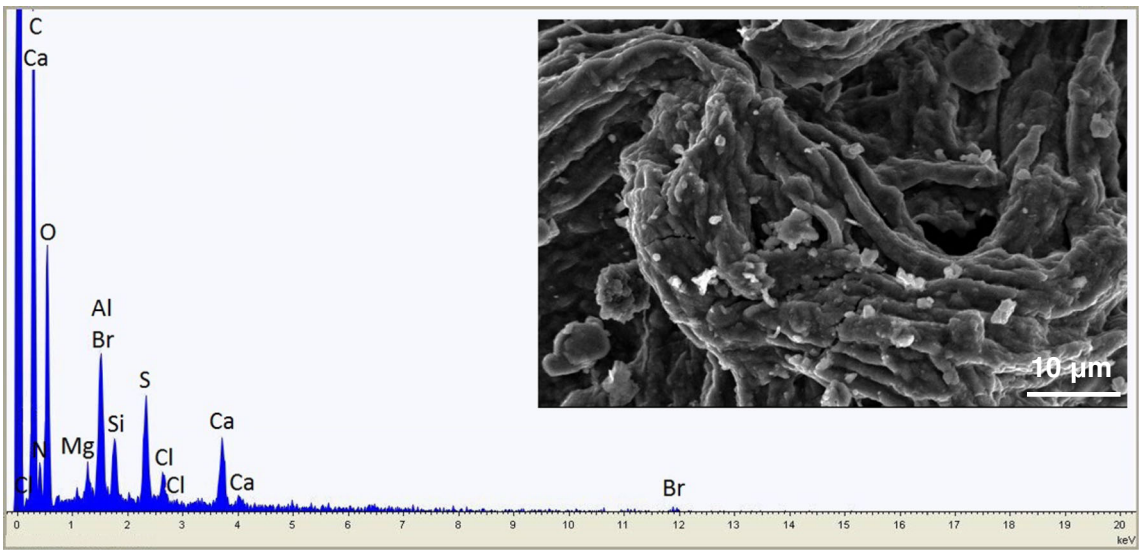

Fig. 8 SEM image of the textile sample dyed in purple and EDX spectrum

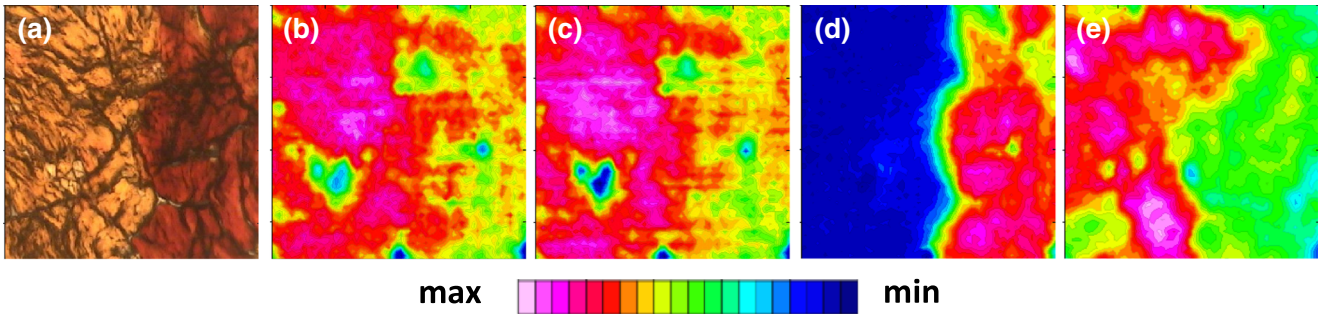

Fig. 9 **a** Visible image in transmission, taken from a region of the purple fibrous archaeological material, which was selected for FTIR imaging in transmission mode, after being pressed with the diamond anvil cell device. FTIR images representing the peak areas at **b** 1540 cm^{-1}, the amide II band of the proteinaceous textile; **c** 1400 cm^{-1}, spatial distribution of sericin; **d** 1314 cm^{-1}, spatial distribution of Tyrian purple; and **e** 1040 cm^{-1}, spatial distribution of kaolinite. The size of the FTIR images is 170×170 μm^2

Mediterranean species (Karapanagiotis et al. 2013). However, the separation of *M. brandaris* and *T. haemastoma* species was not possible (Karapanagiotis et al. 2013). This is confirmed herein by the PCA plot of Fig. 11 which, compared to the previously published report (Karapanagiotis et al. 2013), is enriched with two set of compositional data corresponding to sample T13 which the *M. trunculus* sample was analysed in Fig. 10c and B5 sample analysed elsewhere (Mantzouris and Karapanagiotis 2014).

Figure 11 shows that the PCA scores obtained for the two archaeological samples (paint and textile) are comparable. The data points of both archaeological samples are placed close in the PCA plot and furthermore close to the point of the T13 sample. This is because the relative compositions of

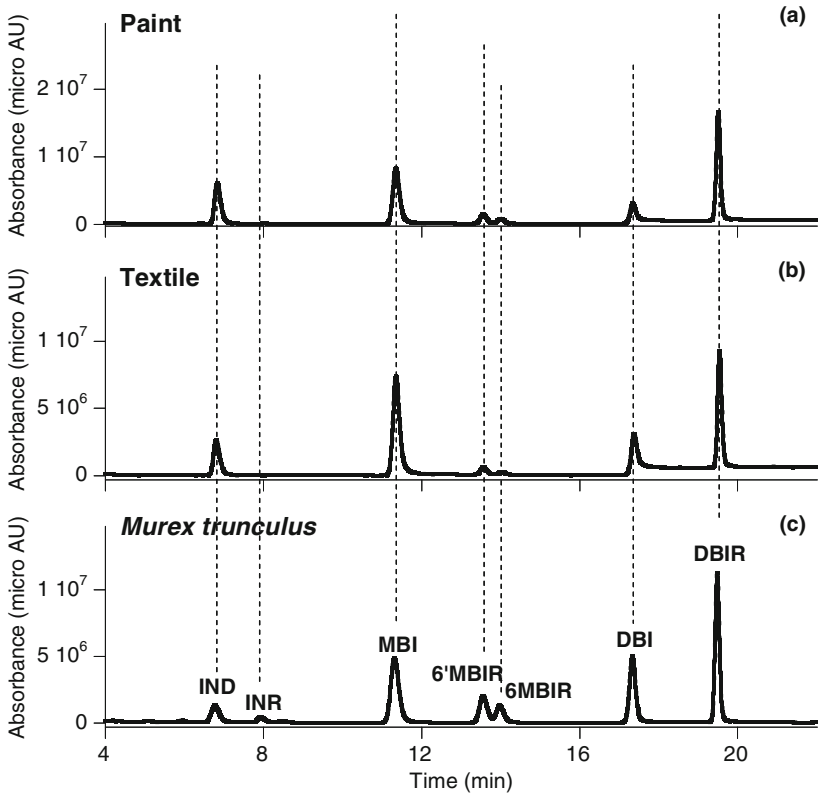

Fig. 10 HPLC chromatograms at 288 nm collected for the **a** paint and **b** textile archaeological samples. **c** The corresponding graph for the *Murex trunculus* sample is included. Relative (%) integrated HPLC peak areas measured at 288 nm for the three samples are described in the table

Sample	IND	INR	MBI	6'MBIR	6MBIR	DBI	DBIR
Paint	19.8	0.1	29.2	4.7	2.3	8.2	35.7
Textile	13.5	0.1	40.3	3.0	0.9	12.3	29.9
Murex trunculus	6.3	1.9	26.3	8.7	4.8	19.8	32.2

Table 1 Relative (%) integrated HPLC (288 nm) peak areas of mollusks and archaeological samples used for the PCA analysis

Sample	IND	INR	MBI	DBI	DBIR	Ref
Murex trunculus						
T1	62.9	1.2	32.1	3.7	0.1	Karapanagiotis et al. 2013
T2	49.8	4.4	37.6	7.1	1.1	Karapanagiotis et al. 2013
T3	35.1	0.4	49.7	14.4	0.4	Karapanagiotis et al. 2013
T4	54.0	1.5	39.4	4.9	0.2	Karapanagiotis et al. 2013
T5	56.0	0.0	37.0	7.0	0.0	Wouters 1992
T6	53.0	14.0	33.0	0.0	0.0	Wouters 1992
T7	4.05	0.0	17.79	60.00	18.16	Koren 2008, 1995
T8	35.2	8.1	30.5	15.8	10.4	Karapanagiotis et al. 2006 and 2013
T9	0.35	0.00	7.41	68.39	23.85	Koren 2008
T10	40.72	3.34	41.33	4.25	10.36	Koren 2008
T11	10.3	2.9	44.4	36.8	5.6	Nowik et al. 2011
T12	27.8	7.5	37.4	23.2	4.1	Karapanagiotis et al. 2013
T13	7.3	2.2	30.4	22.9	37.2	Herein
Murex brandaris						
B1	0.0	0.0	0.0	85.0	15.0	Wouters 1992
B2	0.0	0.0	6.0	81.0	13.0	Wouters 1992
B3	0.0	0.0	1.6	97.2	1.2	Karapanagiotis et al. 2006 and 2013
B4	0.00	0.00	1.36	94.88	3.76	Koren 2008
B5	2.0	0.5	1.8	79.3	16.4	Mantzouris and Karapanagiotis 2014
Thais haemastoma						
H1	0.0	0.0	3.0	91.0	6.0	Wouters 1992
H2	0.0	0.0	3.0	91.0	6.0	Wouters 1992
H3	0.00	0.00	0.86	85.48	13.66	Koren 2008
H4	41.2	0.0	6.0	49.4	3.4	Karapanagiotis et al. 2013
Archaeological samples						
Paint	21.3	0.1	31.4	8.8	38.4	Herein
Textile	14.0	0.1	42.0	12.8	31.1	Herein

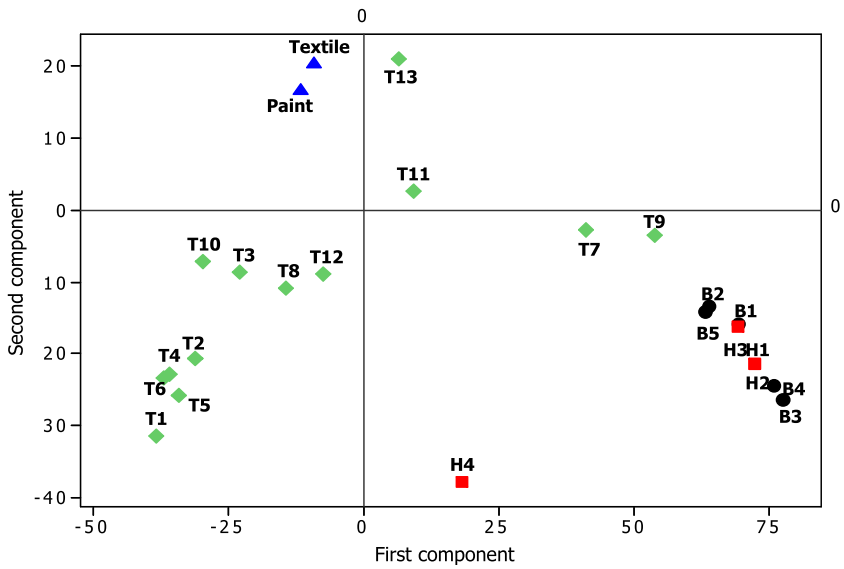

Fig. 11 PCA scores for reference samples of *Murex trunculus* ("T" samples, presented by *green diamonds*), *Murex brandaris* ("B" samples, presented by *black dots*) and *Thais haemastoma* ("H" samples, presented by *red squares*) and archaeological samples (presented by *blue triangles*) using the values of Table 1

the two archaeological samples are similar and not much different from the composition of the T13 sample, as discussed in Fig. 10. Furthermore, the scores for both paint and textile sample fall in a regime which is clearly closer to T (*trunculus*) points than to B (*brandaris*) or H (*haemastoma*) points. This result could be indicative about the source of Tyrian purple used in Daskyleion. However, it must be acknowledged that the relative composition of the archaeological samples could have been affected by degradation processes raised because of ageing and the preparation conditions applied for the production of the painted surface and the dyed textile.

Conclusions

Kaolinite should have been included in the painting and dyeing recipes of Tyrian purple of the fifth century BCE. This conclusion was reached as the molluskan purple and kaolinite were found to co-exist (micro-FTIR, SEM-EDX) in a painted decoration of a burial kline and a textile fragment, both found in the Koru tumulus in Daskyleion.

The results of Fourier transform infrared imaging (FTIRI) suggest that probably the treatment of the textiles fibres with kaolinite constituted a different stage, which might prelude the dyeing process with Tyrian purple. The textile fragment is composed of undyed cotton and silk yarns dyed with the molluskan dye.

The relative compositions of the molluskan materials used in the two archaeological objects are similar according to the HPLC results, which were interpreted using principal component analysis (PCA) taking into account the relative compositions of the extracts of the three Mediterranean mollusks, published in previous reports. It is shown that the PCA scores calculated for the two archaeological samples are close to the corresponding data obtained for *M. trunculus* mollusks.

Acknowledgement The authors would like to thank Dimosthenis Kechagias for his help in the identification of cotton.

References

Andreotti A, Carmignani A, Colombini MP, Modugno F (2006) Characterization of paint organic materials in wall decorations of Macedonian tombs. In: Brecoulaki H (ed) La peinture funeraire de macedoine, emplois et fonctions de la couleur IVe-IIe s av J-C Vol II: planches & tableaux, Appendix IV. National Hellenic Research Foundation, Athens

Cardon D (2007) Natural dyes—sources, tradition, technology and science. Archetype Publications Ltd., London

Clark RJH, Cooksey CJ (1999) Monobromoindigos: a new general synthesis, the characterization of all four isomers and an investigation into the purple colour of 6,6′-dibromoindigo. New J Chem 323–328

Colombini MP, Carmignani A, Modugno F, Frezzato F, Olchini A, Brecoulaki H, Vassilopoulou V, Karkanas P (2004) Integrated analytical techniques for the study of ancient Greek polychromy. Talanta 63:839–48

Cook JG (1993) Handbook of textile fibres I. Natural fibres. Merrow Publishing Co, Wiltshire

Derrick MR, Stulik D, Landry JM (1999) Infrared spectroscopy in conservation science, scientific tools for conservation. The Getty conservation institute, Los Angeles

Friedländer P (1909) Den farbstoff des antiken purpurs aus *Murex brandaris*. Ber Dtsch Chem Ges 42:765–770

Graves PH, Saville BP (1995) Microscopy of textile fibres. Bios Scientific Publishers, Oxford

İren K (2012) Dascyleum. A multicultural society in the shadow of Persia. Curr World Archaeol 54:49–51

İren K (2013) Daskyleion. In: Bagnall RS, Brodersen K, Champion CB, Erskine A, Huebner SR (eds) The encyclopedia of ancient history, 1st ed, Wiley-Blackwell, pp1930–31

Kakoulli I (2002) Late Classical and Hellenistic painting techniques and materials: a review of the technical literature. Rev Conserv 3:56–67

Karapanagiotis I, Sotiropoulou S, Chryssikopoulou E, Magiatis Pr, Andrikopoulos KS, Chryssoulakis Y (2004) Investigation of Tyrian purple occurring in historical wall paintings of Thera. Dyes Hist Archaeol Proceedings of the 23rd DHA meeting, Montpellier, in press

Karapanagiotis I, de Villemereuil V, Magiatis P, Polychronopoulos P, Vougogiannopoulou K, Skaltsounis AL (2006) Identification of the coloring constituents of four natural indigoid dyes. J Liq Chromatogr Relat Technol 29:1491–502

Karapanagiotis I, Mantzouris D, Cooksey C, Mubarak MS, Tsiamyrtzis P (2013) An improved HPLC method coupled to PCA for the identification of Tyrian purple in archaeological and historical samples. Microchem J 110:70–80

Karydas AG (2006) In situ XRF analyses of wall-painting pigments on ancient funeral Macedonian monument. In: Brecoulaki H (ed) La peinture funeraire de macedoine, emplois et fonctions de la couleur IVe-IIe s av J-C vol II: planches & tableaux, Appendix IV. National Hellenic Research Foundation, Athens

Kavkler K, Gunde-Cimerman N, Zalar P, Demsar A (2011) FTIR spectroscopy of biodegraded historical textiles. Polym Degrad Stabil 96: 574–80

Koren ZC (1995) High-performance liquid chromatographic analysis of an ancient Tyrian purple dyeing vat from Israel. Isr J Chem 35:117–24

Koren ZC (2008) Archaeo-chemical analysis of royal purple on a Darius I stone jar. Microchim Acta 162:381–92

Luniak B (1953) The identification of textile fibers. Sir Isaac Pitman & Sons, London

Mantzouris D, Karapanagiotis I (2014) Identification of indirubin and monobromoindirubins in *Murex brandaris*. Dyes Pigm 104:194–96

Mantzouris D, Karapanagiotis I, Valianou L, Panayiotou C (2011) HPLC-DAD-MS analysis of dyes identified in textiles from Mount Athos. Anal Bioanal Chem 399:3065–79

Maravelaki-Kalaitzaki P, Kallithrakas-Kontos N (2003) Pigment and terracotta analyses of Hellenistic figurines in Crete. Anal Chim Acta 497:209–25

Margariti C, Protopapas S, Allen N, Vishnyakov V (2013) Identification of purple dye from molluscs on an excavated textile by non-destructive analytical techniques. Dyes Pigm 96:774–80

McGovern PE, Michel RH (1990) Royal purple dye: the chemical reconstruction of the ancient Mediterranean industry. Accounts Chem Res 23:152–58

Michel RH, Lazar J, McGovern PE (1992a) The chemical composition of the indigoid dyes derived from the hypobranchial glandular secretions of Murex mollusks. J Soc Dyers Colour 108:145–50

Michel RH, Lazar J, McGovern PE (1992b) Indigoid dyes in Peruvian and Coptic textiles of the University Museum of Archaeology and Anthropology. Archeomaterials 6:69–83

Nour WMN, Awad HM (2008) Effect of MgO on phase formation and mullite morphology of different Egyptian clays. J Aust Ceram Soc 44:27–37

Nowik W, Marcinowska R, Kusyk K, Cardon D, Trojanowicz M (2011) High performance liquid chromatography of slightly soluble brominated indigoids from Tyrian purple. J Chromatogr A 1218:1244–52

Serrano A, Sousa MM, Hallett J, Lopes JA, Oliveira MC (2011) Analysis of natural red dyes (cochineal) in textiles of historical importance using HPLC and multivariate data analysis. Anal Bioanal Chem 401:735–43

Sotiropoulou S, Karapanagiotis I (2006) Conchylian purple investigation in prehistoric wall paintings of the Aegean area. In: Meijer L, Guyard N, Skaltsounis AL, Eisenbrand G (eds) Indirubin the red shade of indigo. Life in Progress Editions. Roscoff, pp 71–78

Sousa MM, Melo MJ, Parola AJ, de Melo JSS, Catarino F, Pina F, Cook FEM, Simmonds MSJ, Lopes JA (2008) Flavylium chromophores as species markers for dragon's blood resins from Dracaena and Daemonorops trees. J Chromatogr A 1209:153–61

Westenholz JG, Stolper MW (2002) A stone jar with inscriptions of Darius I in four languages. Arta 005:1–13

Wouters J (1992) A new method for the analysis of blue and purple dyes in textiles. Dyes Hist Archaeol 10:17–21

Wouters J (2001) The dye of *Rubia peregrina*—preliminary investigations. Dyes Hist Archaeol 16(17):145–57

Wouters J, Verhecken A (1989) The coccid insect dyes: HPLC and computerized diode-array analysis of dyed yarns. Stud Conserv 34:189–200

XiaoMei Z, Paul W (2010) Using FTIR spectroscopy to detect sericin on historic silk. Sci China Chem 53:626–31